Computer simulation: Fig. 2 shows a turbo-coded W-CDMA reverse link transmission model. The single mobile user is assumed to continuously transmit information data at 64kbit/s. The data are divided into a sequence of 5120bit data frames. Frame data are first 16bit CRC encoded and then turbo encoded with coding rate of 1/3 and generator polynomials of 1, 5/7, 5/7 in octal notation (the two RSC encoders are the same and have a constraint length of 3 bits (see Fig. 1*a*). A multistage interleaver (termed MIL) [4] realises turbo internal interleaving and channel interleaving. At the W-CDMA transmitter, the coded binary data sequence is transformed into a quaternary phase shift keying (QPSK)-modulated symbol sequence after some non-information bearing data have been appended. Four pilot symbols are appended to the resultant 128ksymbol/s QPSK-modulated symbol sequence every 0.625ms (the time interval beginning with four pilot symbols followed by 76 data symbols is called the time slot) and is QPSK-spread using a 4.096Mchip/s complex long pseudo-random spreading sequence (spreading factor 32) to be transmitted over a frequency-selective fading channel [1]. The fading channel is modelled as a frequency selective Rayleigh channel having an ITU-specified vehicular B power delay profile [5]. Two spatially separated antennas and a four-finger (two fingers/antenna) coherent RAKE combiner are assumed at the base station receiver. Channel estimation for coherent RAKE combining is performed by averaging eight received pilot symbols of two consecutive slots. The RAKE combiner output sample sequence is de-interleaved and turbo decoded as described previously. Signal-to-interference plus background noise power ratio (SIR) measurement based fast transmit power control (TPC) described in [6] is assumed; the power up/down step size is 1dB and the power-control rate is 1600Hz.

We measured the average bit error rate (BER), average received E_b/I_0 per antenna (since the single user is assumed in the simulation, I_0 is equal to the background noise spectrum density N_0), and average number of decoding iterations for various values of target SIR for fast TPC. The measured average BER and the average number of decoding iterations are plotted in Fig. 3 against the average E_b/N_0 per antenna for the fading maximum Doppler frequency f_D = 5 and 80Hz. The maximum number of decoding iterations is eight (in our simulation, after eight iterations, the improvement in BER performance is saturated). It can be clearly seen from Fig. 3 that the introduction of CRC decoding into the turbo decoding iteration process does not degrade the BER performance at all, while the average number of decoding iterations can be reduced by half at average BER = 10^{-4} and by 75% at average BER = 10^{-6}. Similar results were gained under slow fading rates, i.e. f_D = 5Hz.

Conclusions: A method for reducing the average number of iterations has been addressed in this Letter. To reduce the average number of decoding iterations, the CRC error check is incorporated into the decoding iteration process in the turbo decoder and further iterations are stopped when CRC decoding finds that there is no error in the decoded data. Simulations showed that the W-CDMA reverse link suffers no performance degradation even if the average number of iterations is reduced by 75% at BER = 10^{-6} under frequency selective Rayleigh fading.

3 March 1999
Electronics Letters Online No: 19990470
DOI: 10.1049/el:19990470

A. Shibutani, H. Suda and F. Adachi (*Wireless Laboratories, NTT Mobile Communications Network, Inc., 3-5 Hikari-no-oka, Yokosuka-shi, Kanagawa-ken, 239-8536, Japan*)

E-mail: shibu@mlab.yrp.nttdocomo.co.jp

References

1 ADACHI, F., SAWAHASHI, M., and SUDA, H.: 'Wideband DS-CDMA for next generation mobile communications', *IEEE Commun. Mag.*, 1998, **36**, pp. 56–69

2 BERROU, C., GLAVIEUX, A., and THITIMAJSHIMA, P.: 'Near Shannon limit error-correcting coding and decoding: turbo-codes'. Proc. IEEE ICC'93, May Geneva, 1993, pp. 1064–1070

3 FUJIWARA, A., SUDA, H., and ADACHI, F.: 'Turbo codes application to DS-CDMA mobile radio', *IEICE Trans.*, 1998, **E81-A**, pp. 2269–2273

4 SHIBUTANI, A., SUDA, H., and ADACHI, F.: 'Multi-stage interleaver for turbo codes in DS-CDMA mobile radio'. Proc. IEEE APCC/ICCS'98, Singapore, November 1998, pp. 391–395

5 'Procedure for evaluation of transmission technologies for FPLMTS'. ITU-R TG8-1, 8-1/TEMP/233-E, September 1995

6 SEO, S., DOHI, T., and ADACHI, F.: 'SIR-based transmit power control of reverse link for coherent DS-CDMA mobile radio', *IEICE Trans.*, 1998, **E81-B**, pp. 1508–1516

Dual band FSS with fractal elements

J. Romeu and Y. Rahmat-Samii

Experimental and computed results of a frequency selective surface (FSS) based on a certain type of fractal element are presented. The fractal element is a two iteration Sierpinski gasket dipole. Owing to the dual band behaviour of the two iteration Sierpinski gasket dipole, two stopbands are exhibited within the operating frequency band. This behaviour is obtained by arraying one simple element in a single layer frequency selective surface (FSS).

Introduction: The use of certain fractal elements such as the Hubert curve has been proposed for the building of frequency selective surfaces (FSSs) [1]. In this case the space filling properties of certain fractal curves were exploited in order to obtain resonant elements that occupied a small volume. In this Letter we propose making use of the self-similar properties of certain fractal objects to design a dual band FSS. The design of a multiband FSS is usually accomplished by multilayer surfaces or by perturbing the elements or the spacing between elements. One possible approach is to use multiband elements in the construction of the FSS. The multiband properties of antennas designed using fractal shapes have been recently demonstrated [2], and it would appear natural to explore the feasibility of a dual-band FSS based on fractal elements. The FSS is designed by periodically arraying a two iteration Sierpinski dipole. A fundamental constraint of this approach is the band limitation imposed by the excitation of grating lobes. It will be shown that it is possible to array the Sierpinski gasket dipole in such a way that a dual band FSS is obtained. The result is a dual band FSS that has the advantage of comprising a single element and single layer.

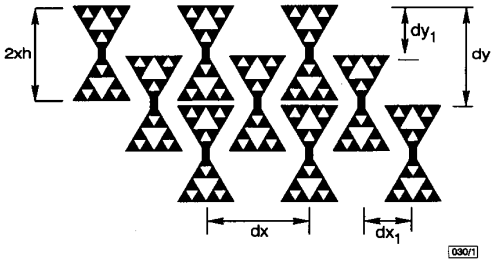

Fig. 1 *Two iteration Sierpinski gasket dipole FSS*

Sierpinski FSS: The multiband behaviour of the Sierpinski dipole has been well described in [2]. Fig. 1 shows the two iteration Sierpinski gasket dipole and the way it has been arrayed to design the FSS. The self-similarity scale factor for the equiangular Sierpinski gasket is 2, and a spacing by a factor of 2 should be expected between resonant frequencies. On the contrary, it is known that for a free standing Sierpinski dipole the first two resonances are spaced by a factor of 3.5. The explanation has to be found in the truncation effect of the first iteration that moves the resonant frequency to lower frequencies. The first and second resonances appear at

$$(2 \times h)/\lambda_1 = 0.306 \qquad (2 \times h)/\lambda_2 = 1.032 \qquad (1)$$

where λ_1 and λ_2 are the wavelengths of the first and the second resonances. For generality throughout this Letter all frequency references have been normalised to the dipole to wavelength ratio.

According to the layout shown in Fig. 1, the spacing between elements is chosen such that

$$dx = dy = 2 \times dx_1 = 2 \times dy_1 \qquad dx = 1.058 \times (2 \times h) \quad (2)$$

For this spatial periodicity, and for normal incidence, four degenerated grating lobes appear with a cutoff wavelength given by

$$\lambda_{cutoff} = \frac{dx}{\sqrt{2}} \quad (3)$$

It is clear from eqns. 1 – 3 that the grating lobes in this structure will appear for

$$(2 \times h)/\lambda_{cutoff} = 1.37 \quad (4)$$

i.e. a frequency above the second resonance of the Sierpinski dipole.

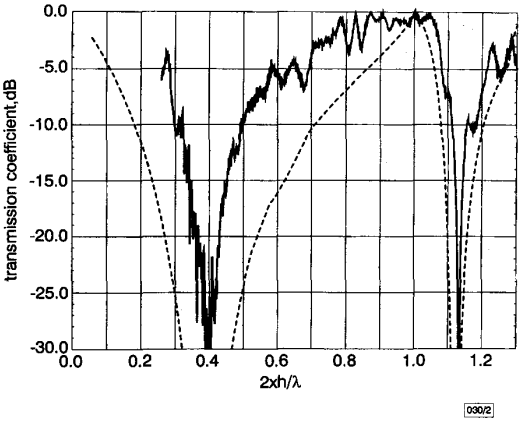

Fig. 2 *Transmission coefficient of Sierpinski FSS*

——— measured results from 2 to 18 GHz
– – – computed results
Note: Frequency scale of measured results has been scaled to take into account frequency shift produced by dielectric backing

Analysis and results: The structure in Fig. 1 has been analysed and the transmission coefficient for an electromagnetic wave with normal incidence to the surface has been computed. The analysis has been carried out with the method of moments for periodic structures with frequency interpolation of the impedance matrix [3]. The results are for an electric field polarised along the axis of the dipoles. In Fig. 2 the computed results for the Sierpinski FSS are presented. The surface clearly exhibits two stop-bands centred at

$$(2 \times h)/\lambda_1 = 0.39 \qquad (2 \times h)/\lambda_2 = 1.12 \quad (5)$$

with a band spacing factor of almost 2.9. These reflection bands appear at a frequency above that which would be expected from eqn. 1. One possible explanation is that the results reported in [2] were obtained with a dielectric backed dipole. Another possible cause could be a shift in the resonance frequency due to the mutual coupling of the different elements. A Sierpinski FSS with 19 by 12 elements (x and y direction) has been built on a 62mil Cu-clad substrate ($\epsilon_r = 2.6$). The height of the element has been chosen to be $2 \times h = 1.95$cm. The transmission properties of the FSS have been measured over the frequency range 2–18GHz. The measurements were performed in an antenna range. The FSS was placed 5cm in front of a linearly polarised wideband ridge horn antenna. The receiving antenna was another linear polarised wideband horn placed at a distance of 5m. The measurement with the FSS was simply calibrated against a measurement in which the FSS was replaced by a 62mil Cu-clad sheet of the same size.

As expected, the measurements exhibit two stop-bands centred at 4.1 and 15.4GHz. These values are approximately shifted down 2GHz from what would be expected from the computed results, and correspond to $2 \times h/\lambda_1 = 0.27$ and $2 \times h/\lambda_2 = 1$. These values are closer to those reported in [2] and shown in eqn. 1 for a single dipole than the values computed and shown in Fig. 2, and eqn. 5 for the FSS. The difference must be attributed to the dielectric backing of the measured FSS. For comparison, for the measured results shown in Fig. 2, the effective electrical permittivity has been empirically determined. It is also noticeable that the measured stop-bands are narrower than predicted. Once again, the presence of the dielectric backing results in an increment in the stored electric energy and a consequent increase in the Q factor of the FSS.

Conclusion: It has been shown that the multiband properties of certain fractal elements, such as the Sierpinski dipole, can be exploited in the design of dual band FSSs. The FSS exhibits two stop-bands with attenuation > 30dB. Although the behaviour of the FSS has only been analysed and measured for normal incidence, at the second stop frequency of 15.4GHz grating lobes appear for an oblique incidence of 22° with respect to normal incidence. Up to a certain degree, it should be possible to modify the ratio between bands by perturbating the shape of the dipole [4].

Acknowledgments: J. Romeu is on sabbatical leave from the Universitat Politecnica de Catalunya, with a NATO Scientific Committee Fellowship. Part of this research has been financed by CICYT and the European Comission through grant FEDER 2FD97-0135. This work has also been supported in part by the US Army Research Office under contract DAAHO4-96-1-0389.

18 March 1999
Electronics Letters Online No: 19990487
DOI: 10.1049/el:19990487

J. Romeu and Y. Rahmat-Samii (*Department of Electrical Engineering, University of California, Los Angeles, 405 Hilgard Avenue, LosAngeles, CA 90095-1594, USA*)

E-mail: rahmat@ee.ucla.edu

References

1 PARKER, E.A., EL SHEIKH, A.N.A., and LIMA, A.C.DE C.: 'Convoluted array elements and reduced size unit cells for frequency-selective surfaces', *IEE Proc. H*, 1991, **138**, (1), pp. 19–22
2 PUENTE, C., ROMEU, J., POUS, R., and CARDAMA, A.: 'On the behavior of the Sierpinski multiband antenna', *IEEE Trans.*, 1998, **AP-46**, (4), pp. 517–524
3 BARLEVY, A.S., and RAHMAT-SAMII, Y.: 'Fundamental constrain on the electrical characteristics of frequency selective surfaces', *Electromagn.*, 1997, **17**, (1), pp. 41–68
4 PUENTE, C., ROMEU, J., BARTOLOME, R., and POUS, R.: 'Perturbation of the Sierpinski antenna to allocate operating bands', *Electron. Lett.*, 1996, **32**, (24), pp. 2186–2188

Chord bisection strategy for fast ellipse location

E.R. Davies

It is shown that a previously proposed rapid sampling technique can be extended using a strategy based on chord bisection. The strategy is characterised by very high speed of operation coupled with accurate location, and can be matched to the level of robustness required by the application. The new technique has been tested on images in which the ellipses are cereal grains with close to 2:1 aspect ratio, but it appears to be suitable for locating ellipses of any eccentricity with near ultimate speed of processing.

Introduction: In many areas of machine vision there is a need for algorithms which operate extremely rapidly, so that huge quantities of input data can be analysed and relevant decisions made in real time. In certain cases, such as the inspection of grain, the problem is exacerbated as large consignments may arrive at a mill, packing station, or ship at irregular intervals, and each will have to be given a bill of health in as little as 3min. This type of situation places extreme pressure on the system designer if cost is to be minimised as well as optimising processing time. For this reason, there is a need for highly efficient algorithms to implement common vision tasks, particularly those related to object location.

The location of elliptical objects involves a considerable computational overhead. Essentially, this is because all the pixels in the image have first to be visited to determine whether they are edge points, and those that are then feed data to Hough transforms or other ellipse detection mechanisms. Recently, an attempt was made to detect objects such as ellipses from their internal regions rather than their boundaries, using a sampling approach which seemed likely to minimise the speed of location [1]. This attempt was highly successful. However, while it was able to locate objects